Chapter 4
Constitutive Model of Coal Mass

4.1 General

The basic objective of the time-dependent constitutive model is to deduce the strength properties of the coal-mass. Many countries such as India, China, the U.S., South Africa, and Australia are practising bord and pillar methods for working. However, limited research has been done in relation to the time-dependent constitutive model for coal-mass. Therefore, back-analysis techniques of field cases of coal pillar have been considered for the estimation of the strength parameters of the proposed time-dependent constitutive model. It has to be estimated for Indian cases. However, due to the lack of well-documented cases, South African cases were utilized for the implementation and validation of the strength parameters of the time-dependent constitutive model. The calibrated material properties of the South African coal caes were considered for extrapolation to Indian cases using Logical Iterative Analysis. The chapter gives a detailed analysis of the implementation of a time-dependent constitutive model.

4.2 Case study

South African bord and pillar coal mines were chosen to implement the proposed time-dependent constitutive model. Although in the literature, many cases were available of South Africa belonging to various coal fields. Similar nature of the coal mines belonging to Nkangala District of Witbank coal fields were considered (Van Der Merwe and Mathey 2013a) for evaluation of strength properties. The collieries considered are New Largo (C-

1), South Witbank (C-2), Blesbok (C-3), Tweefontein (C-4), Koornfontein (C-5) and Waterpan (C-6). The location map of the considered collieries is shown in Fig 4.1. The selected collieries (failed and stable) cases are shown in Tables 4.1 and 4.2. Failed cases have been chosen to evaluate the material properties using the proposed time-dependent constitutive model. Stable cases are chosen for validation of the material properties.

In failed cases, the life of coal pillars was in the range of 1 and 46 years. The depth of the collieries varies between 21.3 m to 90.0 m. The pillars were between 3.2 to 7.5 m wide and 1.52 to 4.88 m height. In stable cases, the depth of the collieries varies between 18.58 m to 91.44 m. The pillars were between 2.91 to 7.62 m wide and 1.19 to 2.78 m height. Some of the stable reported cases do not show the date of mining; this might be due to old mines. Based on the reported data, the expected age of the stable cases more than 60 years has been considered, so for validation, 60 years was considered. These cases were found stable till year 2013 (Van Der Merwe and Mathey 2013b).

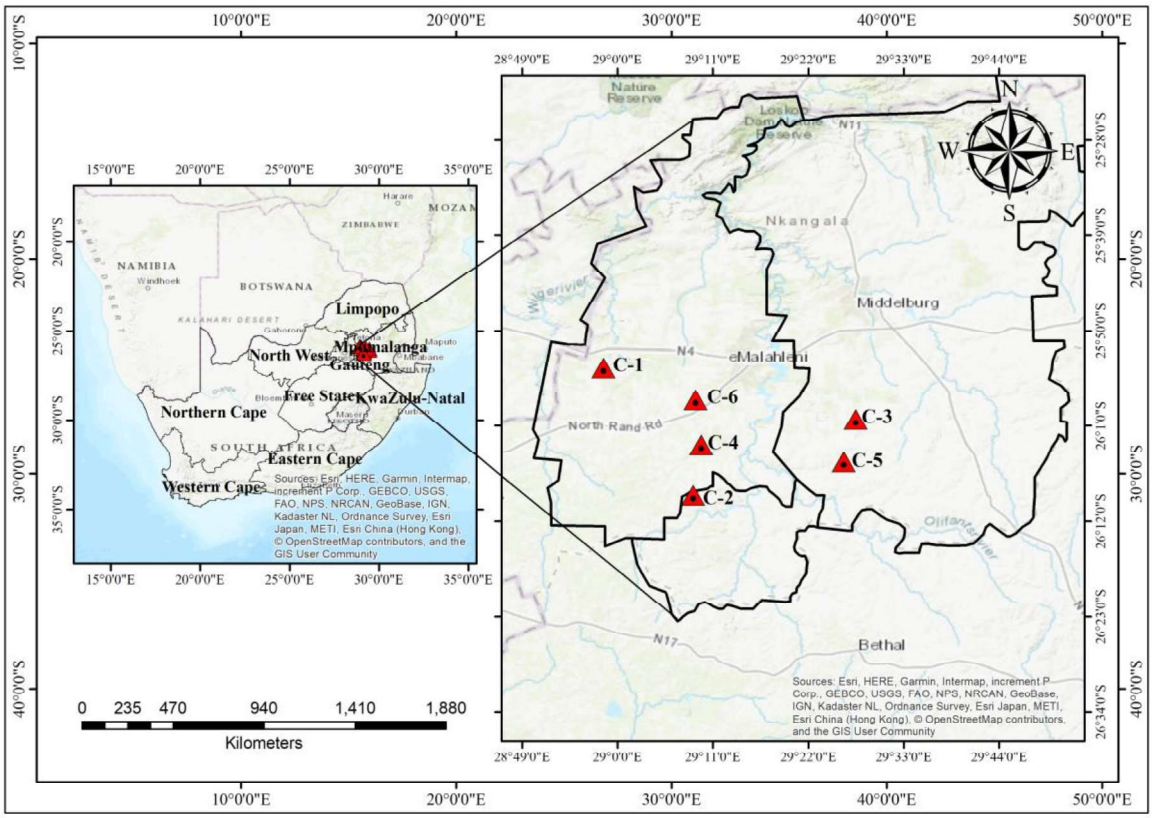

Figure 4.1: Map showing the locations of Witbank coalfields (https://www.diva-gis.org/gdata)

Table 4.1: Failed pillar database

Failed pillar cases									
Case No	**Name of the Colliery**	**Location mark on map**	**Depth (m)**	**Pillar width (m)**	**Gallery width (m)**	**Pillar height (m)**	**Date of mining**	**Date of collapse**	**Age of the pillar (Years)**
1	New Largo	C-1	32	3.3	6.4	2.3	1954	2000	46
2	New Largo		34	3.5	6.7	2.7	1953	1971	18
3	New Largo		32.5	3.2	6.5	2.1	1954	1991	37
4	New Largo		34	3.5	6.7	2.7	1952	1968	16
5	South Witbank	C-2	56	5.1	6.5	3.3	1957	1976	19
6	Blesbok	C-3	68.6	3.35	5.79	1.52	1954	1955	1
7	Tweefontein	C-4	62	6.1	6.1	4	1930	1976	46
8	Tweefontein		62	6.1	6.1	4	1930	1968	38
9	Koornfontein	C-5	88.4	7.16	6.55	4.88	1958	1962	4
10	Koornfontein		90	7.5	6	4.8	1958	1968	10
11	Waterpan	C-6	61	6.1	6.1	4.57	1932	1964	32
12	Waterpan		57.9	6.1	7.62	3.96	1932	1964	32

Table 4.2: Stable pillar database

Stable pillar cases till 2013									
Case no	**Colliery**	**Mark on map**	**Depth (m)**	**Pillar Width (m)**	**Gallery width (m)**	**Pillar height (m)**	**Date of mining**	**Date of monitoring**	**Age of the pillar till 2013 (Years)**
1	Blesbok	C-3	25.98	3.11	5.53	1.34	NR	2013	60*
2	Blesbok		26.83	2.91	5.09	1.33	NR	2013	60*
3	Blesbok		42.61	4.38	5.07	1.61	NR	2013	60*
4	Blesbok		23	4	5.68	1.58	NR	2013	60*
5	Blesbok		23.76	4.3	5.21	1.5	NR	2013	60*
6	Blesbok		23.54	4.24	5.38	1.54	NR	2013	60*
7	Blesbok		26.75	4.54	4.97	1.65	NR	2013	60*
8	Blesbok		19.4	4.26	5.22	1.4	NR	2013	60*
9	Blesbok		20.8	4.24	5.18	1.38	NR	2013	60*
10	Blesbok		23.33	4.37	5.08	1.33	NR	2013	60*
11	Blesbok		45.72	4.27	5.49	1.19	NR	2013	60*
12	Blesbok		68.58	5.18	5.49	1.19	NR	2013	60*
13	Blesbok		91.44	6.1	5.49	1.19	NR	2013	60*
14	Blesbok		76.2	7.62	6.1	1.37	NR	2013	60*
15	New Largo	C-1	39.1	6.63	6.36	2.6	1978	2013	35
16	New Largo		36.5	7.25	6.3	2.68	1984	2013	29
17	New Largo		24.15	6.1	6.25	2.65	1981	2013	32
18	New Largo		25.7	6.15	6.17	2.6	1983	2013	30
19	New Largo		18.58	4.86	6.16	2.78	1970	2013	43
20	New Largo		21.5	5.09	5.96	2.75	1969	2013	44
21	New Largo		44.95	5.03	6.01	2.68	1965	2013	48
22	New Largo		26.51	4.32	6.68	2.65	1967	2013	46

4.3 Numerical simulation

In recent years, numerical simulation techniques have become primary study methods in geotechnical engineering for dealing with complex geo-mining conditions. FDM-based numerical simulation techniques are used to study time-dependent strength deterioration and predict the pillar's life. The considered case study was used to deduce the material properties and the simulation results were also validated with field observations.

4.3.1 Model preparation

All the pillar model is prepared in three layers: roof, coal seam, and floor, as per geometry mentioned in Tables 1 and 2. A typical case no 7 of (table 4.1) of failed cases is demonstrated here. The pillar measures 6.1 m in width, 6.1 m in length, and 4 m in height, while the gallery's width is about 6.1 m. The model was discretised with an element size of 0.4 m × 0.4 m × 0.6 m. During the preparation of the model, the galleries were assigned with different group to null it to form a pillar. The floor and roof are considered elastic, whereas the coal pillar is considered a time-dependent Hoek-Brown strain-softening material. The finite difference method is used to simulate all the cases mentioned in Tables 4.1 and 4.2 using FLAC^{3D}. Fig.4.2a shows the three-dimensional view of the model without nulling the galleries. The galleries were extracted/nulled to form a pillar, as shown in Fig. 4.2b. Fig. 4.2b illustrates the three-dimensional view and sectional view of a typical case, number 7 of Table 4.1.

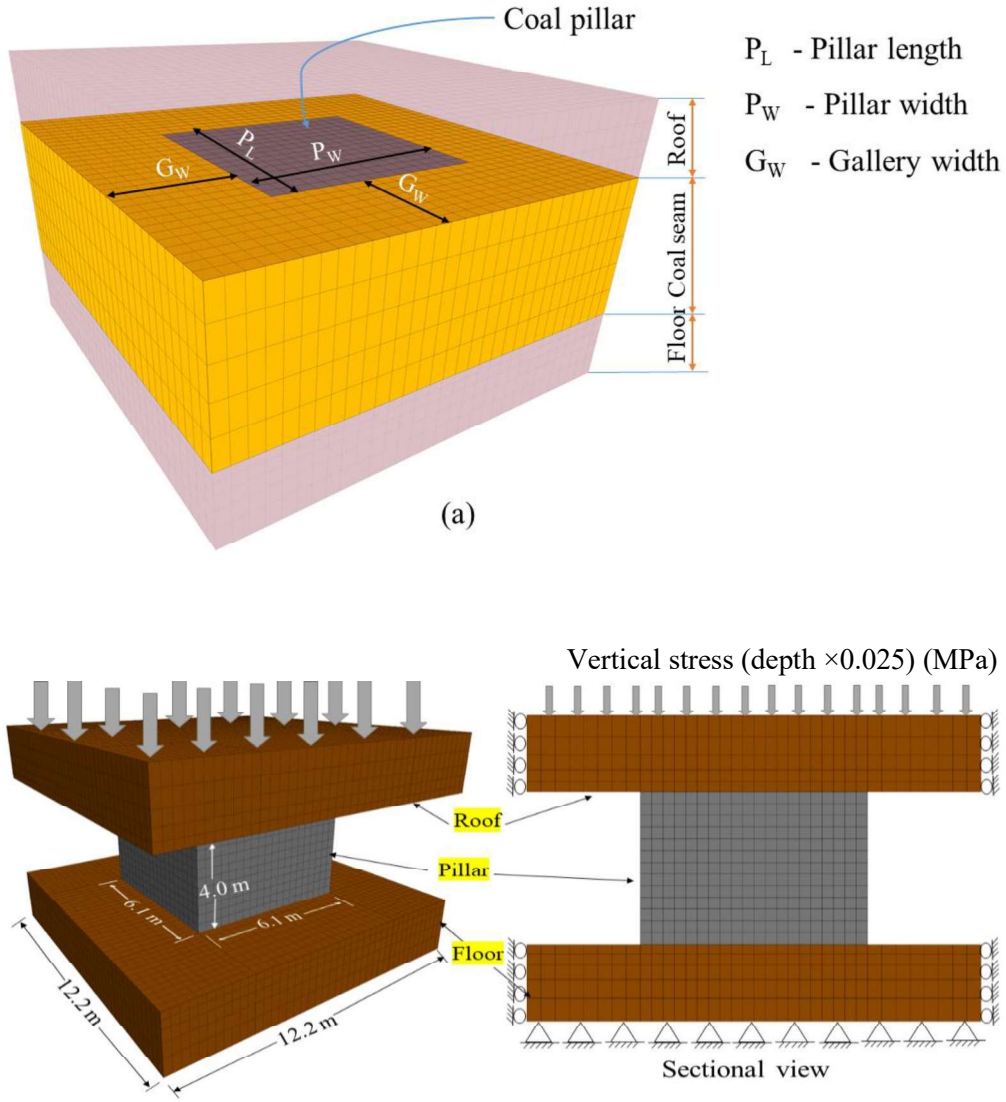

Figure 4.2: Three-dimensional discretization of the model (case no. 7 of failed cases)

The model's X and Y directions are assigned with roller boundaries, whereas the bottom of the model in the Z direction is restricted. A vertical stress of (depth × 0.025) MPa is applied from the model top. The proposed constitutive model is assigned to the model, and back analysis techniques are used to deduce the material's properties. The simulation procedure and the calibration of material properties were explained in detail in the next subsequent sections.

4.3.2 Calibration of material properties

All the field cases of the coal pillar mentioned in Section 4.2 (failed and stable) are simulated considering the time-dependent constitutive model. The cases considered from Witbank Coalfield have 12 failed and 22 stable cases. It is to be noted that in-situ testing of coal pillars or laboratory testing of large-size specimens provides a better strength parameter, but these are costly and time-consuming. Therefore, a standard back-analysis technique for calibrating coal-mass properties for the proposed time-dependent constitutive model. The proposed constitutive model has strength properties m and s for crack/yield initiation, peak and residual. The prime objective of this section is to estimate these parameters through the back-analysis technique of coal pillar cases by satisfying the failed and stable cases. Various permutations and combinations of the material properties were considered. The range of crack/yield strength properties m_c is taken from 1.2 to 1.5, s_c is taken from 0.1 to 0.05, ultimate peak strength properties m_p is taken from 1 to 2, and s_p is taken from 0.1 to 0.001. Similarly, the range of residual strength properties m_r is taken from 0.1 to 0.2 and s_r from 0.0001 to 0.000015. The peak reduction parameter β was taken from 0.00001 to 0.0001, and the softening parameter α ranged from 100 to 300. The UCS of the Witbank coalfield was taken from the literature (Mathey 2015) i.e. the average UCS of specimens with 60 mm diameter was 21.43MPa, but the intact and residual strength properties were derived based on testing 25 mm diameter samples. Therefore, the UCS for 25 mm diameter is calculated based on the expression (see equation 4.1) suggested by (Darlington et al. 2011).

$$\sigma_{cd} = \sigma_{c50}\left(\frac{50}{d}\right)^{0.22} \quad \text{---------- (4.1)}$$

Where d is the diameter, σ_{c50} is the UCS of 50 mm diameter samples. All the cases of coal pillars have been simulated for each combination of strength properties. The

error in the predicted life with actual life has been calculated for each case. The variance of the errors of all the cases has then been calculated. The similar approach has been adopted for each permutation and combination of the strength properties. The best-fit strength properties have been chosen based on the minimum variance in the error (i.e., the difference between actual age and predicted age). The combination of strength properties in which the variance gets minimum variance and predicted life less than the actual life (i.e. almost near to actual life and not more than the actual life) is considered the best-fit combination. This phenomenon is considered mainly for the better design of the pillars. The calibrated strength properties obtained from the simulation analysis are shown in Table 4.3

Table 4.3: Rock-mass properties of coal pillar, floor and roof

S. no	Material	Density (kg/m^3)	E (GPa)	Hoek-Brown time-dependent strength parameters					
				m_c	s_c	m_p	s_p	m_r	s_r
1	Coal	1300	2	1.47	0.01	1.55	0.073	0.125	0.00001
2	Floor/Roof	2500	5	-	-	-	-	-	-

The predicted pillar life based on the deduced material properties was compared with the actual life of the pillar, as shown in Fig. 4.3. From the bar chart (shown in Fig. 4.3), the red bars show the field observation data, and the green bars show the numerical simulation results. The comparison of the predicted life and actual life of the failed cases shows that except for case number 8, in all cases, the predicted life is almost near or less than the actual life. The average axial strain value with time has also been plotted. Fig. 4.4 shows the average axial strain v/s age of some of the pillar curves of failed cases (case no 1, 3, 5, 7, 8 and 12) of Witbank coalfields. Failed cases show an exponential increment in average axial strain with time. The uncontrolled increment in average axial strain indicates the failure of the pillar. At this stage, the model becomes un-equilibrium.

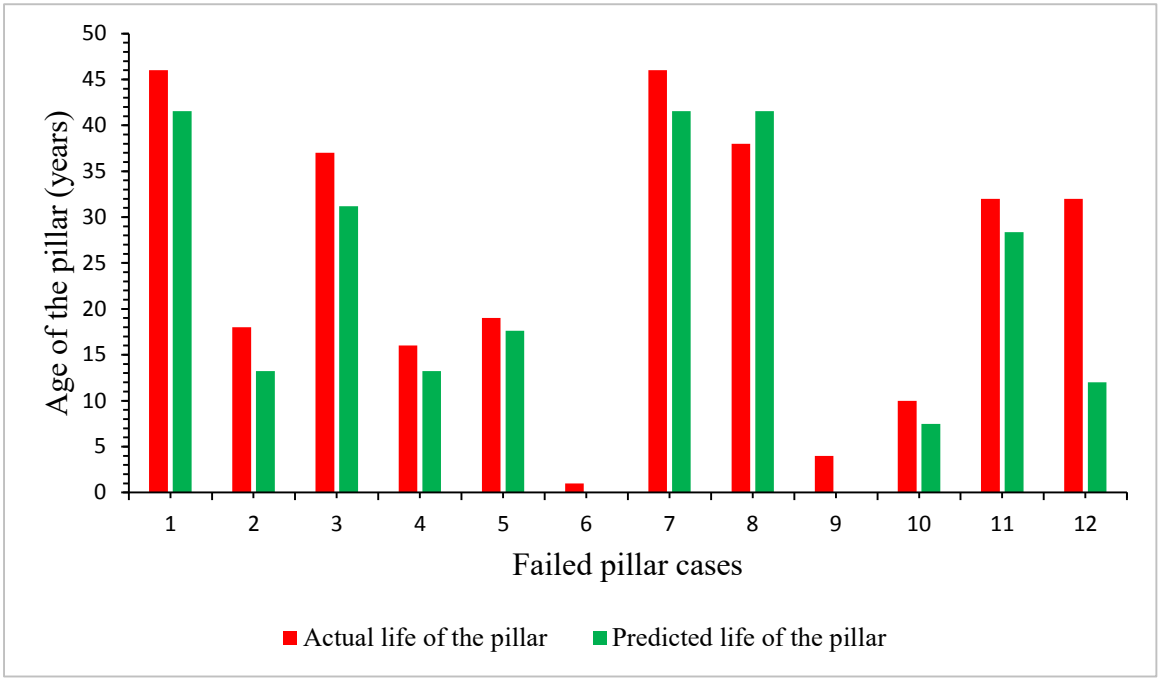

Figure 4.3: Comparison of predicted life and actual life of the pillars

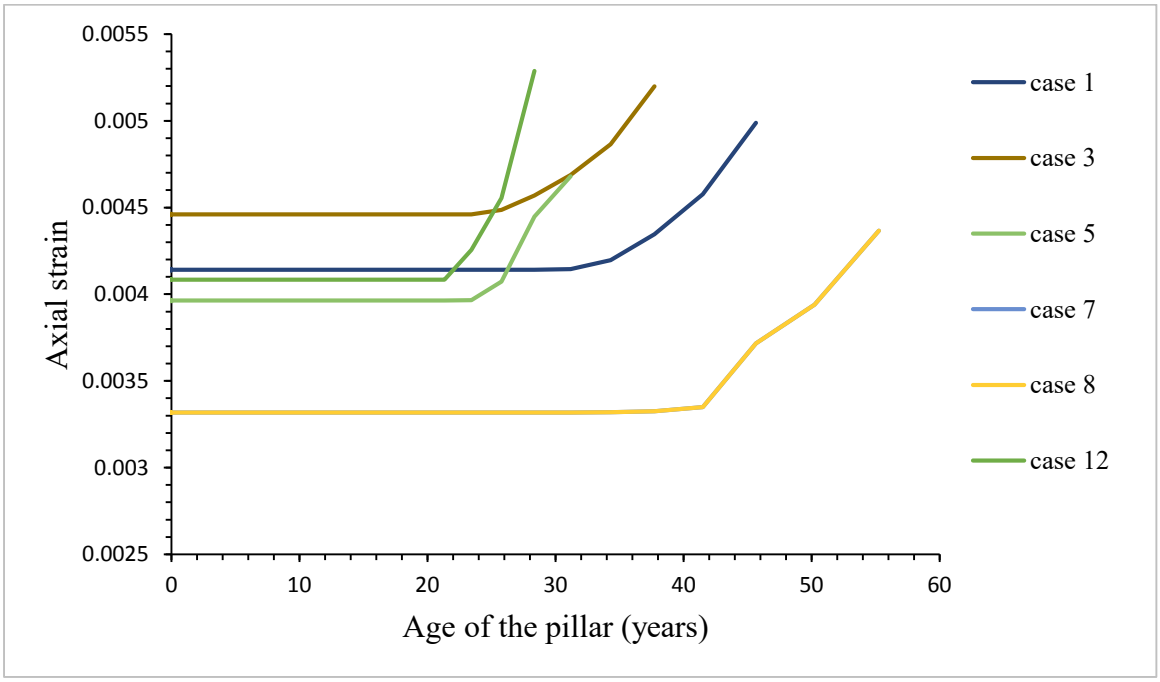

Figure 4.4: Axial strain vs age of the pillar curves of failed cases of Witbank coalfields

The calibrated rock mass properties were validated by considering stable cases from the same collieries. Validation was conducted in terms of average axial strain increment in the pillar with increasing age. Fig. 4.5 shows the graphical representation of some stable cases in terms of the average axial strain v/s age of the pillar. It is observed

in Fig. 4.5 that most of the cases exhibited a constant average axial strain with the age of the pillar. Constant axial strain with time indicates no creep developed up to this age. However, some cases exhibit a slight increment of axial strain with time, yet they also show stable behaviour, indicating the development of creep while maintaining stability. The results concluded that the strength parameters obtained from the failed cases of the Witbank coalfield were validated by the stable cases from the same coal fields.

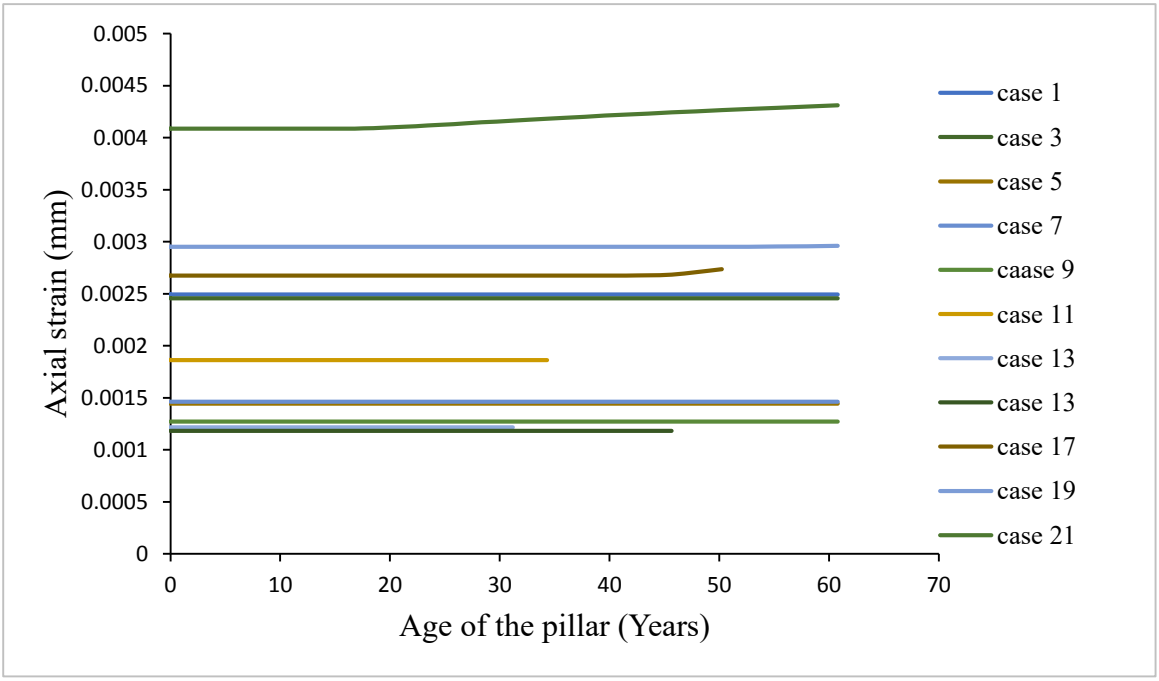

Figure 4.5: Axial strain v/s age of the pillar curves of stable cases of Witbank coalfields

4.4 Results and Discussions

The proposed time-dependent constitutive model was used to monitor pillar behaviour. This includes the vertical stress contour, vertical stress profile, and increment of average axial strain with the age of the pillar. All the cases (mentioned in Tables 4.1 and 4.2) were simulated with time. The life of the pillar was estimated when all the elements were yielded and an un-equilibrium condition occurred. The results are explained in detail by considering one failed and one stable case in the following sub-sections.

4.4.1 Failed case

Among 13 failed cases, case no 7 of the pillar was chosen to explain the behaviour of the pillar age. It was observed that the yielding starts from the outer region and moves towards the core of the pillar with age. Fig. 4.6 shows the change in vertical stress within the pillar (case no 7) at different simulation ages. In Fig. 4.6, the red colour indicates the high-stress value, whereas the blue colour indicates the low-stress value. The top of the model represents the roof, and the bottom is the model's floor. After the pillar formation, in 1 day, the edges showed maximum stress, as shown in Fig. 4.6a. From the simulation results, it was observed that with the increasing age of the pillar, the low-stress region increased on the sides of the pillar as shown in Fig. 4.6. The increasing low-stress region on the pillar's sides is due to the yielding of elements. Because of the yielding of the elements, the load on the outer region (crushing zone) is transferred into the plastic zone area, and as a result, the plastic zone area shows maximum induced stress. As the age of the pillar increased from 1 day (after formation) to 15,159 days (41.53 years), the low-stress region on the pillar's sides also increased. As a result, the adjacent zone elements (plastic zone) experienced maximum vertical stress. Fig. 4.7 shows the vertical stress contour at the middle level of the pillar from 1 day to 15,159 days (41.53 years) of extraction. In the middle level of the pillar, because of the more yielding, it shows high stress. The simulation results showed that the pillar of case no 7 is completely yielded at 15,159 days (41.53 years).

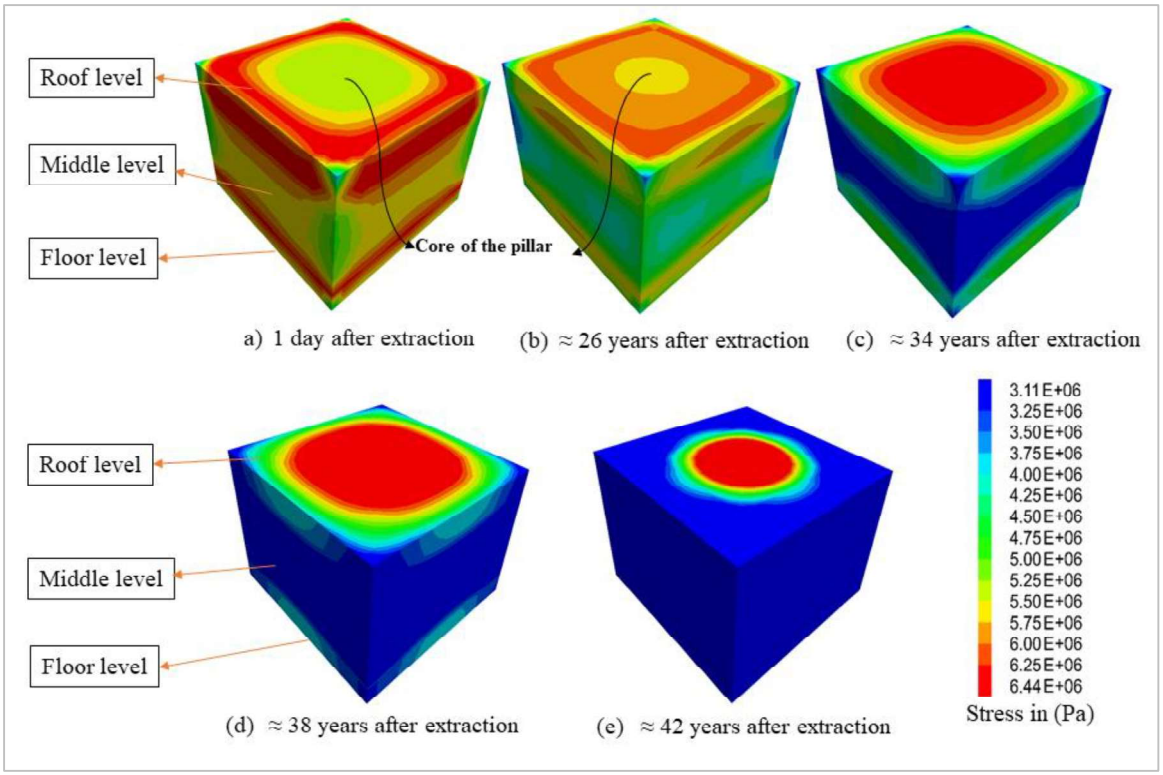

Figure 4.6: Vertical stress contour at different ages of the pillar

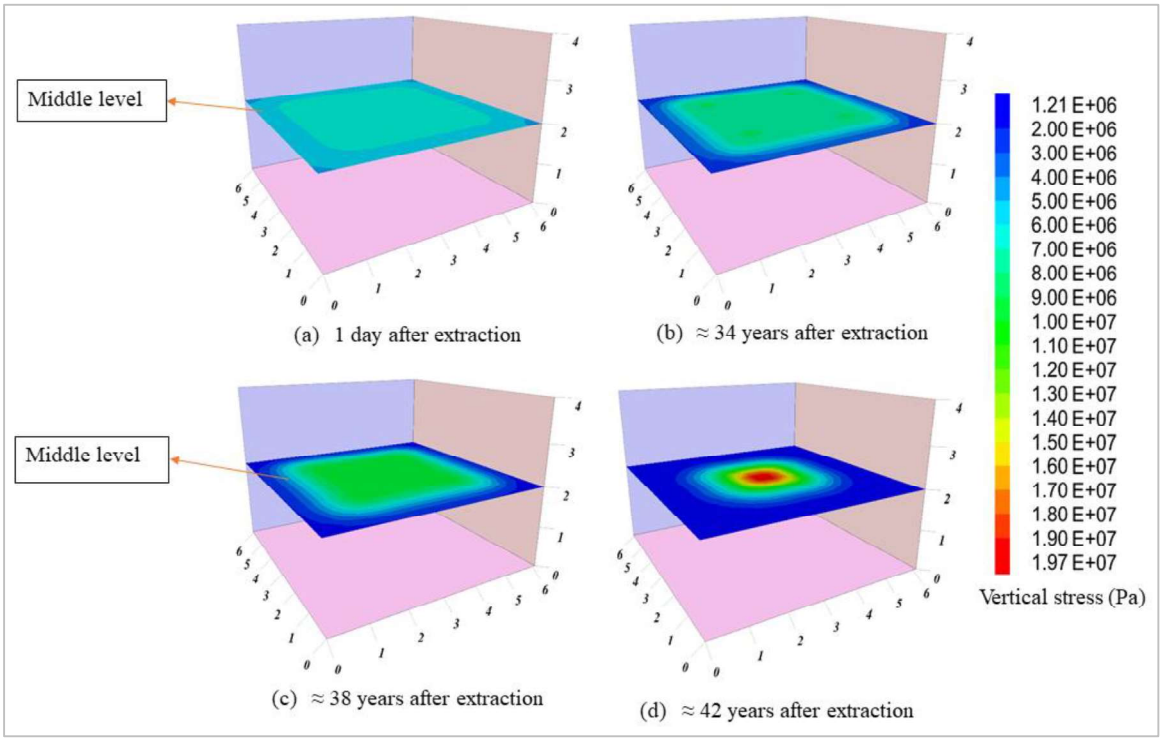

Figure 4.7: Vertical stress contour at the middle level of the pillar

Fig. 4.8 (for case no 7) shows the shape of the vertical stress profile at the middle level of the pillar with age increment. Fig. 4.8a shows the combined vertical stress profile at different ages, whereas Fig.4.8b, c, d and e show the individual vertical stress profiles at different ages. After the development of the pillar, the average vertical stress observed was about 6.45 MPa (i.e. equivalent to tributary area stress). This stress remains the same during its life. The simulation results showed no noticeable change in the distance of the low-stress region (crushing zone) from both ends of the pillar until 12,528 days (34.32 years) of extraction. However, an increase in vertical stress was observed. After 12,528 days (34.32 years) passed, the low-stress region (crushing zone) extended to 1.31 m, and vertical stress increased to 8.2 MPa. At this stage, as seen in Fig. 4.8c, the pillar's core (centre portion) has a vertical stress of around 7.87 MPa. After 13,781 days (37.75 years) of extraction, the low-stress region is further extended deeper into the pillar up to a distance of 1.75 m with a maximum vertical stress of 9.59 MPa, and the core of the pillar shows a vertical stress of 9.35 MPa (Fig. 4.8d). After 15,159 days (41.53 years) passed, the low-stress region further extended deeper into the pillar. The pillar completely yielded by forming an inverted V-shape stress curve, as shown in Fig. 4.8e. Before the pillar's complete yielding, the core of the pillar bears an extremely high stress of approximately 19.5 MPa (Fig. 4.8e). This was mainly because of the stress transfer from the crushing zone (yielded zones). In all the stages from day 1 to 15,159 days (41.53 years), an increase in the crushing zone is observed. From Fig. 4.8, it was observed that the stress profile shape with increasing pillar age (or with increasing crushing zone) changed from an M-shape to an inverted V-shape. At the age of 15,159 days (41.53 years), the model gets un-equilibrium and fails. It doesn't have the strength to sustain tributary area stress.

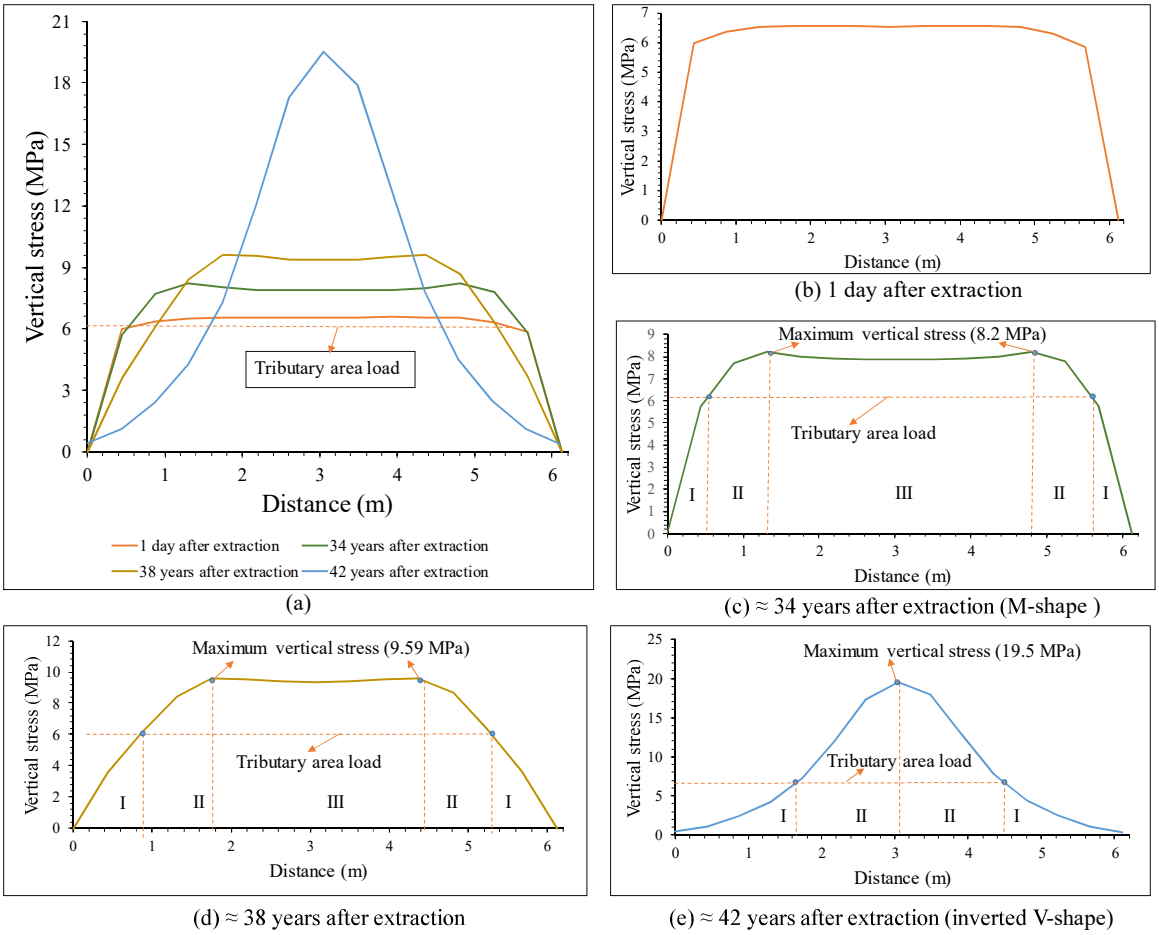

Figure 4.8: Stress profile at the middle level of the pillar with time increment (case no 7; at average vertical stress of 6.2 MPa

The average axial strain v/s age of the pillar has also been plotted. Fig. 4.9 shows the graphical representation of axial strain with the age of the coal pillar (case 7 of Table 4.1). The results show no noticeable change in the average axial strain, which was observed up to 7,779 days (21.31 years). After 7,779 days (21.31 years), an exponentially increasing trend in axial strain was observed. After 15,159 days (41.53 years), the pillar was completely yielded, and an uncontrolled continuous sharp increase in the average axial strain was observed. Fig. 4.8a, b, c, and d shows the plastic strain increment within the pillar with increasing age. The red shade in Fig. 4.8a, b, c, and d shows the zero/negligible plastic strain, and the blue shade shows the maximum plastic strain. Zero/negligible plastic strain shows the elastic region of the pillar, whereas plastic strain indicates the pillar's crushing and plastic zone region. The simulation results revealed that

even after the yielding of sides and corners of the pillar, no noticeable axial and plastic strain was observed up to the age of 7,779 days (21.31 years). With further increasing the age of the pillar, the plastic strain (plastic zone area) moves towards the pillar's core, resulting in a reduction in the elastic zone area of the pillar.

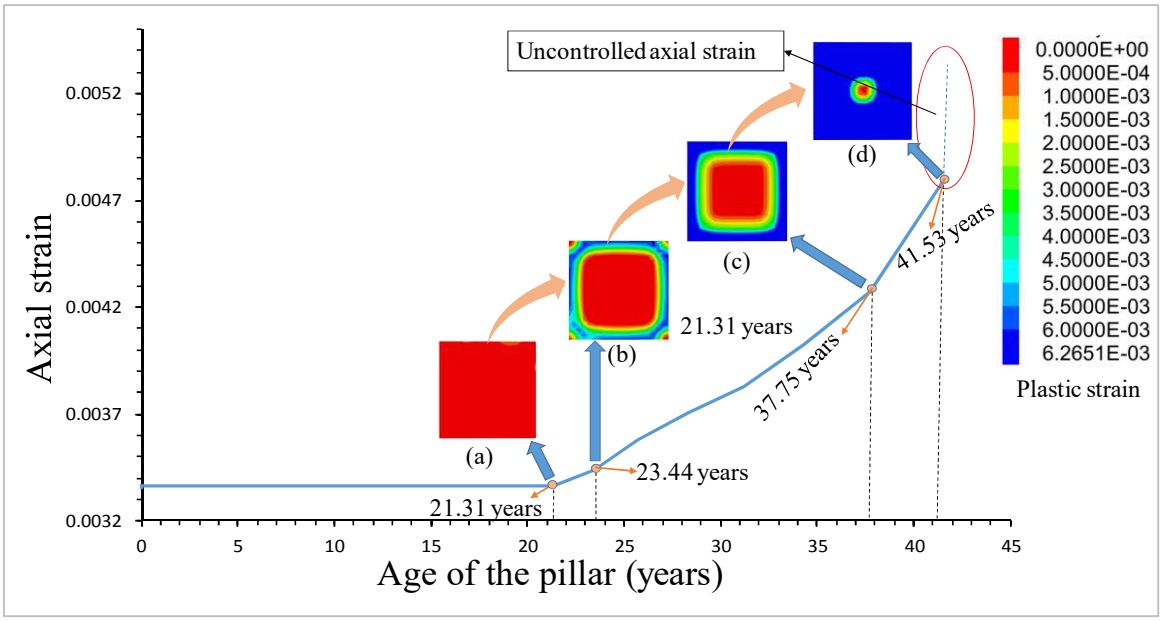

Figure 4.9 Graphical representation of average axial strain with age of the pillar and plastic strain (case no 7)

4.4.2 Stable cases

All the stable cases (as in Table 4.2) were simulated. It was observed that all the cases showed stable behaviour. The lowest w/h ratio case (case no 22 from Table 4.2) is considered to explain the behaviour of the pillar with age. Fig. 4.9 shows the vertical stress contour at different ages of the pillar. The model was simulated up to the age of 46 years. The simulation results showed no noticeable change in the vertical stress observed from 1 day after extraction to 46 years after extraction, as shown in Fig. 4.9 a & b.

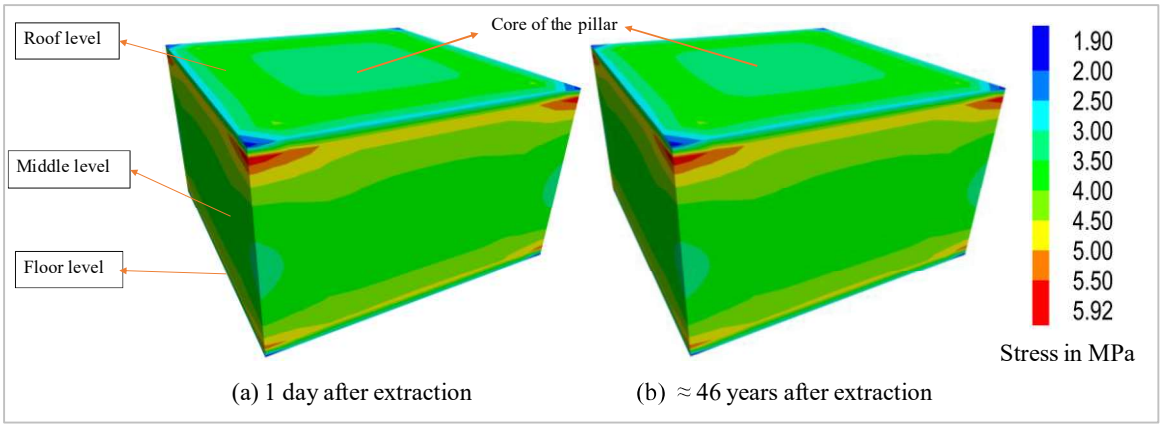

Figure 4.10: Vertical stress within the pillar with increasing age

The stress profile in the middle section of the pillar also aboserved, as shown in Fig. 4.10. From the stress profile, it was observed that from 1 day to 45.6 years after extraction, the observed stress profile was almost equal to the tributary load of the pillar, as shown in Fig. 4.10a and b. The stress profile of the simulation results will not show a V-shaped curve after 45.6 years of extraction, which indicates the stability of the pillar.

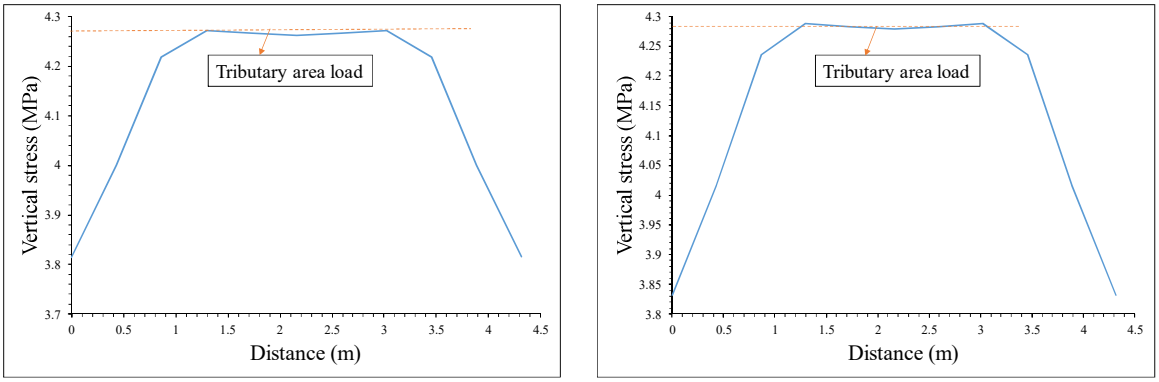

(a) 1 day after extraction (b) ≈ 46 years after extraction

Figure 4.11: Vertical stress profile within the pillar at the middle level (case no 22) at average vertical stress of 4.27 MPa

4.5 Pillar strength formula

An attempt has also been made to develop the pillar strength formula with respect to age based on the statistical analysis of the results of numerical simulation techniques. Total 31 cases (including the original Witbank cases) have been considered for the estimation of the coal pillar age. The details of the cases are given in Table 4.4.

Table 4.4 Cases simulated for evaluating the pillar strength

Case no	Depth (m)	Pillar width (m)	Bord width (m)	Mining height (m)	Tributary area stress (MPa)	Predicted age (years)
1	25.90	3.66	8.53	3.05	5.75	4.21
2	24.61	3.66	8.53	3.05	5.46	16.01
3	22.02	3.66	8.53	3.05	4.88	34.32
4	34.00	3.5	6.70	2.7	5.78	13.23
5	32.30	3.5	6.70	2.7	5.49	10.93
9	61.00	6.1	6.10	4.57	4.88	28.36
10	67.10	6.1	6.10	4.57	5.37	14.55
11	70.15	6.1	6.10	4.57	5.61	7.46
12	32.00	3.3	6.40	2.3	5.53	41.53
13	35.20	3.3	6.40	2.3	6.08	19.37
14	36.80	3.3	6.40	2.3	6.36	12.02
15	75.14	7.16	6.55	4.88	5.51	13.23
16	32.50	3.2	6.50	2.1	5.97	31.2
17	35.75	3.2	6.50	2.1	6.57	10.93
18	37.38	3.2	6.50	2.1	6.87	2.87
19	62.00	6.1	6.10	4	4.96	41.53
20	68.20	6.1	6.10	4	5.46	23.44
21	71.30	6.1	6.10	4	5.70	16.01
22	58.90	6.1	6.10	4	4.71	50.2
23	52.70	6.1	6.10	4	4.22	80.93
24	57.90	6.1	7.62	3.96	5.86	12.02
25	55.01	6.1	7.62	3.96	5.57	19.37
26	49.22	6.1	7.62	3.96	4.98	41.53
27	56.00	5.1	6.50	3.3	5.79	17.61
28	53.20	5.1	6.50	3.3	5.50	25.78
29	90.00	7.5	6.00	4.8	5.83	7.46
30	85.50	7.5	6.00	4.8	5.54	16.01
31	76.50	7.5	6.00	4.8	4.96	37.75

Statistical analysis was carried out to formulate pillar strength as a function of age. With increasing age of the pillar, at some point just before pillar failure the strength of the pillar becomes equal to the tributary area stress. Thus, the ultimate strength of the pillar was considered as a tributary area stress at the time of failure of the pillar. This phenomenon was considered to derive the time-dependent pillar strength formula. Salamon and Munro's (MDG and Munro. A.H. 1967) pillar strength formula derived for South African cases has a dimensional factor $\left(\frac{w^{\alpha}}{h^{\beta}}\right)$. Therefore, the life of the pillar, along with the rate of tributary stress and dimensional factor for all the cases, has been plotted. From the statistical analysis, a pillar strength formula as a function of w (pillar width), h (pillar height), and age of the pillar (A) was established (Fig. 4.11).

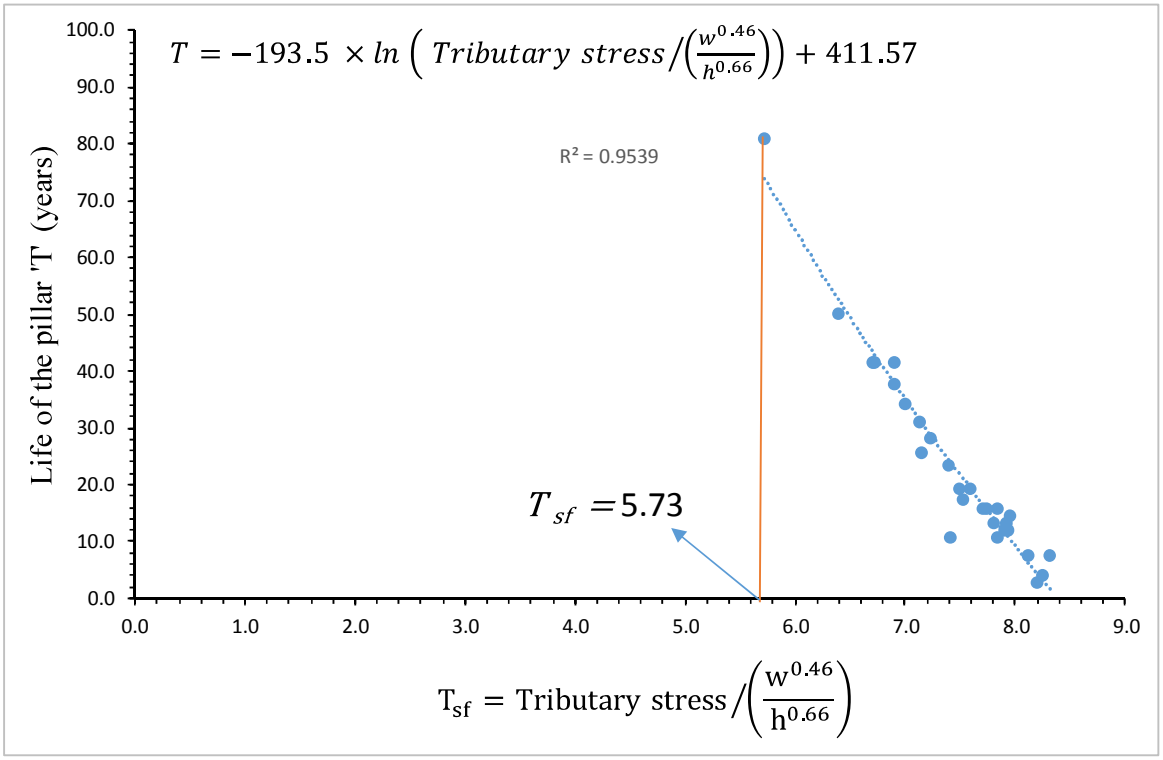

Figure 4.12: Relation between T_{sf} with respect to the life of the pillar

From the statistical analysis, the best fit obtained to calculate the life of the pillar (T) is

$$T = 411.57 - 193.5 \times \ln\left(\frac{Tributary\ stress}{\left(\frac{w^{0.46}}{h^{0.66}}\right)}\right) \text{---------- (4.2)}$$

The strength of the pillar at age 'A' will be estimated by rearranging equation 4.2. It is to be noted that the strength of the pillar is equal to the stress of the tributary area. In this stage, 'A' becomes 'T'. The strength of the pillar equation is

$$Strength_A = \frac{w^{0.46}}{h^{0.66}} \times e^{\left(\frac{411.57-A}{193.5}\right)} (MPa) \quad \text{if } T_{sf} > 5.73 \text{---------- (4.3)}$$

Where "w is the width of the pillar (m), h is the pillar height (m) A is the age of the pillar (years). The suggested pillar strength equation is only applicable when $T_{sf} > 5.73$. Below this value (i.e. $T_{sf} > 5.73$), the pillar does not undergo crack/yielding initiation, so it shows long-term stability.

4.6 Constitutive model for Indian cases

The constitutive model was initially developed for Indian cases; however, South African cases were utilised for validation and implementation due to the lack of well-documented cases. The model and results were validated using these cases, and once validated, the calibrated material properties of the South African coal cases were considered for extrapolation to Indian cases using Logical Iterative Analysis. Extrapolating the time-dependent constitutive model's material properties from South African to Indian coal cases is a comprehensive process that requires initial parameter estimation and iterative refinement. This iterative approach involves rigorous numerical simulations and validation with field data, ensuring that the adapted model accurately predicts the time-

dependent constitutive model input parameters of coal pillars under Indian conditions. A methodology was considered to ensure the strength equivalence by calculating the pillar strength of the same cases by using pillar strength formulas suggested for India and South African coal fields for baseline comparison. In the first step, the strength parameters of both the formulas are normalised to get constant strength values of the considered cases. This process involves adjusting the parameters to get equivalent pillar strengths.

The pillar strength formula, as per equation 4.3 for an age of 30 years for South African cases, was considered, which has a strength factor and geometrical factor, as shown in equation 4.5. Whereas for Indian cases, a similar nature strength formula was considered so that it is easy for a base line comparison. The considered strength formula for Indian cases must satisfy the failed and stable pillar cases, i.e. all the failed cases must have a FOS<1.0, and stable cases must have a FOS >1.0.

$$S = 7.2 \times \left(\frac{w^{0.46}}{h^{0.66}}\right) \text{---------- (4.4)}$$

Adjusted Salamon and Munro (1967) formula:

$$S = UCS_{inch} \times 0.277 \times \left(\frac{w^{0.46}}{h^{0.66}}\right) \text{---------- (4.5)}$$

Where h is the height of pillar (m), w is the width of the pillar (m), and UCS_{25} is the intact UCS of the 25 mm size sample.

While developing this formula, it was observed that the UCS of Indian cases (failed and stable) was deduced by considering a 1 inch^3 coal sample. The strength of South African UCS was deduced for a 25 mm diameter coal sample having an L/D ratio of 2.5 to 3.0. Therefore, a primary study was done to deduce the UCS for 25 mm size coal samples for Indian cases. From the literature, it was observed that there is a shape and size effect on the UCS of a sample. To estimate the shape effect, the UCS of the coal

samples with different L/D ratios are tested in the laboratory. Table 4.5 shows the details of the samples tested, and Fig. 4.12 shows the graphical representation of strength with the L/D ratio of the samples.

Table 4.5: Coal samples tested

Sample	Dia (mm)	Length (mm)	Load (kg)	L/D	Strength (MPa)
1	47.27	46.62	3870	0.98625	22.06328138
2	47.15	52.425	4200	1.11188	24.06668311
3	47.155	69.68	4400	1.47768	25.20736914
4	47.04	89.285	4600	1.89807	26.48216876
5	47.103	93.34	4800	1.98161	27.55969735

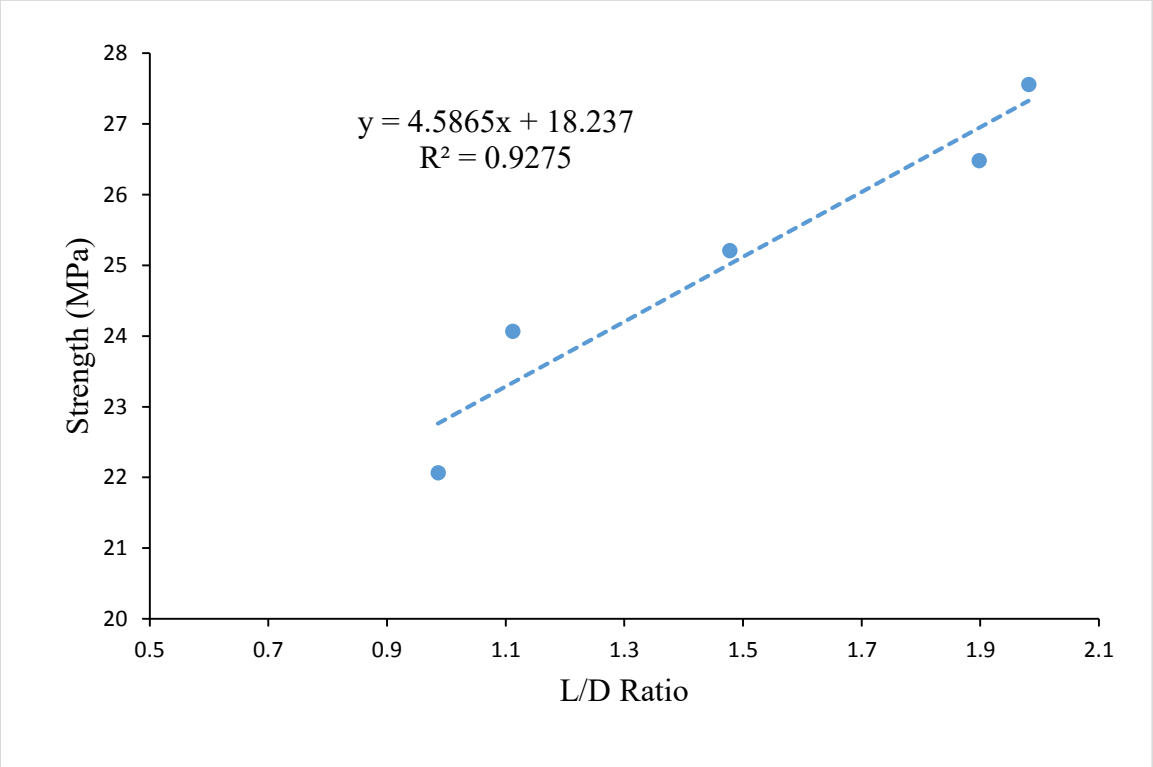

Figure 4.13: Strength v/s L/D ratio graph

The strength equation from the graph (Fig. 4.12) was modified so that it will match with the Bieniawski pillar strength formula.

$$Strength = 22.823 \times \left(0.2 \times \frac{W}{D} + 0.8\right) \text{ ---------- (4.6)}$$

The equation is a combination of the strength and the geometrical factors. From the literature, it was observed that the length-to-diameter (L/D) ratio for a sample in a uniaxial compressive strength (UCS) test should be between 2.5 and 3. From this, the shape factor for the 1 inch^3 sample (i.e. L/D = 1) was calculated as 0.88. After calculating both shape and size effects, the suggested pillar strength formula for failed and stable Indian cases is mentioned in Tables 4.6 and 4.7 (Murali Mohan et al. 2001) as follows.

$$S = UCS_{25\,mm} \times 0.25 \times \left(\frac{w^{0.46}}{h^{0.66}}\right) \text{---------- } (4.6)$$

Table 4.6: Failed cases of Indian coal mines

Case no.	Mines (Seam)	D (m)	h (m)	w (m)	B (m)	w/h	σc (MPa)
1	Amritnagar (Nega Jamehari)	30	4.5	3.6	5.7	0.8	45
2	Amritnagar (Nega Jamehari)	30	6	3.6	5.4	0.6	45
3	Begonia (Begonia)	36	3	3.9	6	1.3	26
4	Amlai (Burhar)	30	5.4	4.5	4.5	0.8	25
5	Sendra Bansjora (X)	23	8.1	4.65	5.55	0.6	24
6	W. Chirimiri (Main)	90	3.75	5.4	6	1.4	45
7	Birsingpur (Johilla top)	129	3.6	7.5	6	2.1	38
8	Pure Kajora (Lower Kajora)	54	3.6	5.4	6	1.5	33
9	Pure Kajora (Lower Kajora)	56	3.6	4.95	6.45	1.4	33
10	Shankarpur (Jambad bottom)	42	4.8	4.5	4.5	0.9	47
11	Ramnagar (Begunia)	70	1.8	2.85	3.15	1.6	26
12	Ramnagar (Begunia)	51	1.8	3	3.6	1.7	26
13	Kankanee (XIII)	160	6.6	19.8	4.2	3	27
14	Kankanee (XIV)	140	8.4	18.6	5.4	2.2	25

Table 4.7: Stable cases of Indian coal mines

Case no.	Mines (Seam)	D (m)	h (m)	w (m)	B (m)	w/h	σc (MPa)
1	Bellampalli (Rossi)	36	3	5.4	6	1.8	48
2	Nimcha (Nega)	48	6	9.9	6	1.7	50
3	Morganpit (Salarjung)	270	3	8.1	3.6	2.7	46
4	Ramnagar (Ramnagar)	75	2.7	9.9	6.6	3.7	28
5	Lachhipur (Lower Kajora)	38	5.1	7.2	3.9	1.4	33
6	N. Salanpur (X)	30	5.1	9	6	1.8	21
7	Bankola (Jambad top)	102	4.8	10.1	2.4	2.1	35
8	Bankola (Jambad top)	75	3	6.3	4.2	2.1	35
9	Surakacchar (G-I)	106	3.5	16	4	4.6	29
10	Lachhipur (Lower Kajora)	38	5.1	18.3	4.2	3.6	33
11	E. Angarapatra (XII)	30	2.1	6	6	2.9	19
12	Kargali Incline (Kathara)	36	3.6	9.3	5.7	2.6	40
13	Jamadoba 6 and 7 Pits (XVI)	80	2	5.8	5.5	2.9	29
14	Topsi (Singharan)	85	1.8	7	3.9	3.9	41

Pillar strength generally depends on rock mass *UCS* and the geometry of the pillar. Based on this hypothesis, the pillar strength formula estimated for South African cases (equation 4.4) should give the same strength while using the pillar strength formula estimated for Indian cases (equation 4.6). The pillar strength calculated by using the South African pillar strength formula having an intact UCS of 26 MPa is equivalent to the pillar strength calculated by using the Indian pillar strength formula having an intact UCS of 28.8 MPa.

Based on the strength equivalence, a hypothesis was considered that the rock mass strength of the South African coal pillar having a UCS of 26 MPa is equivalent to the Indian coal pillar with a UCS of 28.8 MPa. Hoek-Brown failure criterion was considered to extrapolate the rock mass properties as follows.

$$\sigma_3 + \sigma_{ciSA}(m_{bSA} \times \frac{\sigma_3}{\sigma_{ciSA}} + S_{SA})^a = \sigma_3 + \sigma_{ciIND}(m_{bIND} + \frac{\sigma_3}{\sigma_{ciIND}} + S_{IND})^a \text{--------- (4.7)}$$

$$\sigma_{ciSA}^2 \times \left(\frac{m_{bSA} \times \sigma_3}{\sigma_{ciSA}}\right) + (\sigma_{ciSA}^2 \times S_{SA}) = \sigma_{ciIND}^2 \times \left(\frac{m_{bIND} \times \sigma_3}{\sigma_{ciIND}}\right) + (\sigma_{ciIND}^2 \times S_{IND}) \text{------ (4.8)}$$

From the above equation equating the coefficients of the strength parameters (m and s)

$$\sigma_3 \times (m_{bSA} \times \sigma_{ciSA}) = \sigma_3 \times (m_{bIND} \times \sigma_{ciIND}) \text{ ---------- (4.9)}$$

$$(\sigma_{ciSA}^2 \times S_{SA}) = (\sigma_{ciIND}^2 \times S_{IND}) \text{ ---------- (4.10)}$$

There fore

$$m_{bIND} = \frac{m_{bSA} \times \sigma_{ciSA}}{\sigma_{ciIND}} \text{ ---------- (4.11)}$$

$$S_{IND} = \left(S_{SA} \times \left(\frac{\sigma_{ciSA}}{\sigma_{ciIND}}\right)^2\right) \text{ ---------- (4.12)}$$

Where σ_{ciSA} is the intact *UCS* of South African coal mass, σ_{ciIND} is the intact UCS of Indian coal mass, (m_{bSA} and S_{SA}) are the Hoek-Brown strength properties of South African coal mass and (m_{bIND} and S_{SIND}) are the Hoek-Brown strength properties of Indian coal mass. Considering these values in equations 4.9 and 4.10, strength properties for Indian coal mass have been deduced. The deduced strength parameters are peak strength properties (m_p and s_p) 1.39 and 0.059, crack initiation strength properties (*mc* and *sc*) 1.32 and 0.008, residual

strength properties (m_r and $s_{r)}$ 0.11 and 0.000008, and the softening parameters considered are α = 200 and β = 0.000195.

The extrapolated time-dependent strength parameters from south African coal mass to Indian coal mass were also tried to validate by considering failed Indian cases from the literature. Although the age of the pillars was not mentioned, a hypothesis of 30 years of age was considered for failed cases. 15 Indian failed cases were simulated by using the proposed time-dependent constitutive model with the deduced material properties. Table 4.8 shows the failed Indian cases with simulated life of the pillar.

Table 4.8: Failed Indian cases with simulated life of the pillar

Case no.	Mines (Seam)	Simulated life (years)
1	Amritnagar (Nega Jamehari)	44.6
2	Amritnagar (Nega Jamehari)	25.18
3	Amritnagar (Nega Jamehari)	30.472
4	Begonia (Begonia)	5.47
5	Amlai (Burhar)	53.3
6	Sendra Bansjora (X)	32.5
7	W. Chirimiri (Main)	1.3
8	Birsingpur (Johilla top)	0
9	Pure Kajora (Lower Kajora)	25.181
10	Pure Kajora (Lower Kajora)	3.73
11	Shankarpur (Jambad bottom)	Stable
12	Ramnagar (Begunia)	0
13	Ramnagar (Begunia)	17.199
14	Kankanee (XIII)	0
15	Kankanee (XIV)	1.443

Statistical analysis was carried out to formulate pillar strength as a function of age. With the increasing age of the pillar, at some point just before pillar failure, the strength of the pillar becomes equal to the tributary area stress. Thus, the ultimate strength of the pillar was considered as a tributary area stress at the time of failure of the pillar. This phenomenon was considered to derive the time-dependent pillar strength formula. The pillar strength formula (see equation 4.3) derived for South African cases has a dimensional factor $\left(\frac{w^{\propto}}{h^{\beta}}\right)$. Therefore, the life of the pillar, along with the rate of tributary stress , dimensional factor and UCS for all the cases, has been plotted. From the statistical analysis, a pillar strength formula as a function of *w* (pillar width), *h* (pillar height), age of the pillar (*A*), and UCS was established (Fig. 4.13).

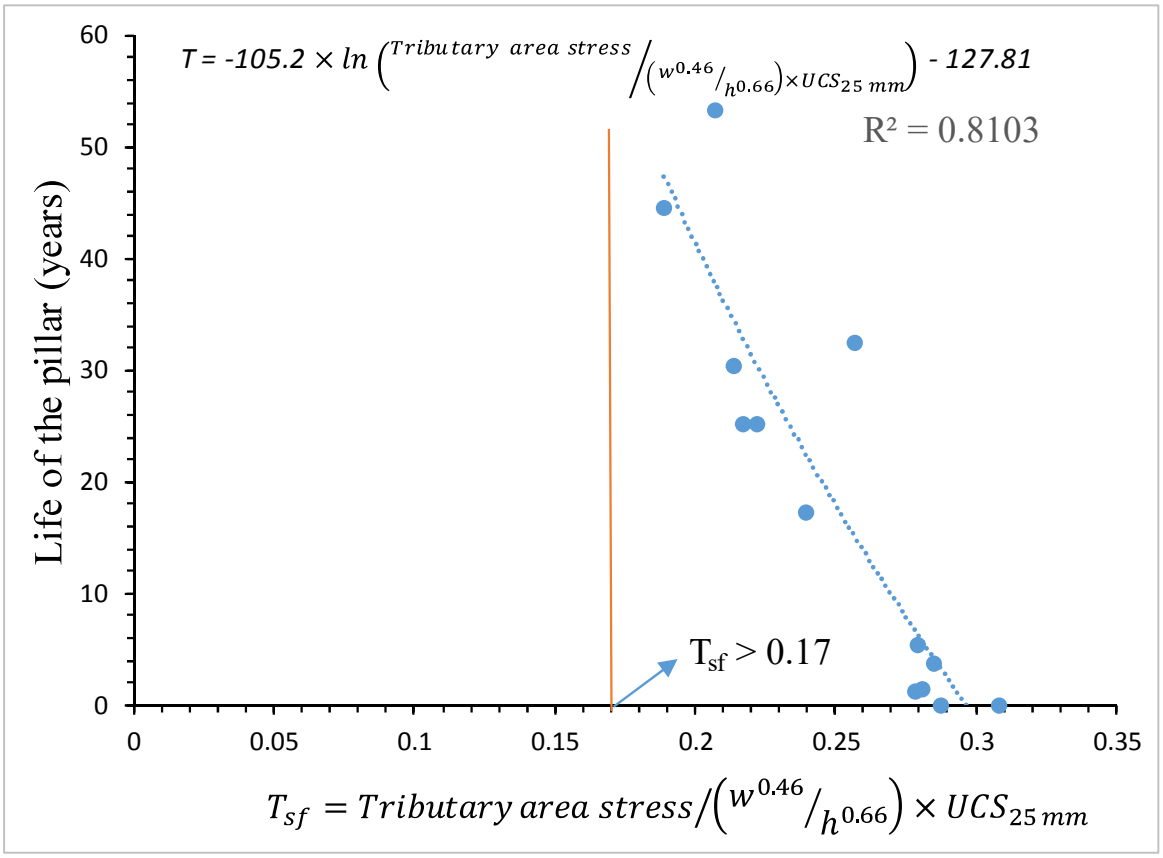

Figure 4.14: Relation between T_{sf} with respect to the life of the pillar

From the statistical analysis, the best fit obtained to calculate the life of the pillar (T) is

$$T = -105.2 \times ln\left(\frac{Tributary\ area\ stress}{\left(w^{0.46}/h^{0.66}\right)\times UCS_{25\ mm}}\right) - 127.81 \text{ ---------- (4.13)}$$

The strength of the pillar at age 'A' will be estimated by rearranging equation 4.13. It is to be noted that the strength of the pillar is equal to the stress of the tributary area. In this stage, 'A' becomes 'T'. The strength of the pillar equation is

$$Strength_A = UCS_{25\ mm} \times \frac{w^{0.46}}{h^{0.66}} \times e^{-\left(\frac{A+127.81}{105.2}\right)} \text{ ; for } T_{sf} > 0.17 \text{ ---------- (4.14)}$$

Where "w is the width of the pillar (m), h is the pillar height (m) A is the age of the pillar (years). The suggested pillar strength equation is only applicable when $T_{sf} > 0.17$. Below this value (i.e. $T_{sf} > 0.17$), the pillar does not undergo crack/yielding initiation, so it shows long-term stability.

4.7 Concluding remarks

South African bord and pillar coal mines were chosen to implement the proposed time-dependent constitutive model. Back analysis techniques were considered to deduce the strength properties of the Witbank coalfield. The relevant strength parameters are crack initiation strength properties $m_c = 1.47$ and $s_c = 0.01$, ultimate peak strength parameters $m_p = 1.55$ and $s_p = 0.073$, residual parameters $m_r = 0.125$ and $s_r = 0.0000$, softening parameter $\alpha = 200$ and peak reduction parameter $\beta = 0.00065$. The validation was carried out with stable cases in the same coalfield (Witbank). The simulation results of almost all the stable cases showed a constant average axial strain with negligible increment with time, indicating the pillar's stability (the coal pillar's strength is more than the stress acting on a pillar). After the deduced strength parameters of South African coal fields were validated, a logical approach was considered to extrapolate to Indian coal field cases. The

deduced strength parameters are peak strength properties (m_p and s_p) 1.39 and 0.059, crack initiation strength properties (*mc* and *sc*) 1.32 and 0.008, residual strength properties (m_r and $s_{r)}$ 0.11 and 0.000008, and the softening parameters considered are α = 200 and β = 0.000195. These deduced strength parameters are validated by considering failed Indian cases. A pillar strength equation with age was proposed by statistical analysis of the results obtained from the simulation for South African and Indian coal fields. The simulation results are obtained in terms of average axial strain with increasing age of the pillar. The proposed constitutive model is suitable for estimating the life of the pillar. It will be highly beneficial for predicting post-failure disasters, such as subsidence.